

PACS 78.67.-n, 78.55.-m

Optical and photoluminescent properties of Ag/Al₂O₃ nanocomposite films obtained by pulsed laser deposition

E.G. Manoilov

*V. Lashkaryov Institute of Semiconductor Physics, NAS of Ukraine
41, prospect Nauky, 03028 Kyiv, Ukraine
E-mail: dept_5@isp.kiev.ua*

Abstract. The method of pulsed laser deposition in vacuum from forward and backward particle flows from an erosion torch was used to prepare silver films and Ag/Al₂O₃ nanocomposite films. Measured were transmission and time-resolved photoluminescence spectra. The authors studied the influence of conditions for film formation on their optical and photoluminescent properties. For the first time, there observed was luminescence with quantum energy 1.6 eV and relaxation times up to several microseconds.

Keywords: nanocomposite film, metal in oxide matrix, time-resolved photoluminescence, local surface plasmon resonance, pulsed laser deposition.

Manuscript received 25.05.09; accepted for publication 14.05.09; published online 30.06.09.

1. Introduction

Silver nanoparticles (NP), clusters and composite nanostructures based on them demonstrate local surface plasmon resonance (LSPR) [1-3], luminescence in the visible spectral range [2-8], photochromism [2], which opens wide possibilities to study distinctive optical properties of nanoparticles as compared to those in bulk objects as well as to use them in various applications from biosensors to informatics and storage devices. Excitation of LSPR results in creation of strong local fields around the nanoparticles, which causes enhancement of Raman scattering, luminescence, optical non-linearity, etc. To observe luminescence enhanced by plasmons, Ag NP are more preferable than Au NP due to lower contribution of interband transitions to the imaginary part of dielectric function [9-11].

Up to date, obtained were silver nanoparticles and clusters, bands of local (interface) surface plasmon absorption of which cover a wide spectral range from visible up to near infra-red regions. Using the methods of electron lithography, arrays of silver nanostructures with dimensions of hundreds nanometers were formed on SiO₂ substrate [9]. Ag NP and clusters were reduced from silver oxides by using ultra-violet irradiation or thermal processing [4-6]. 2D Ag NP arrays with dimensions about 10 nm in amorphous silicon were deposited using electron-beam evaporation [9]. Developed also were the ways to prepare metal-dielectric composites, the so-called nanocermet, by ion implantation, sol-gel technologies, magnetron sputtering

of targets, etc. Prepared were glasses with Ag NP [3, 9], also formed were Ag NP in TiO₂ matrix [2, 7, 8]. There are only single works where the method of pulsed laser deposition (PLD) was used to prepare thin nanocomposite films containing Ag nanocrystals embedded into Al₂O₃ matrix [12, 13]. In [12], the authors used the method of spectroscopic ellipsometry to determine the effective complex refraction index versus the silver concentration in Al₂O₃ film. Considered in [13] was desorption of xenon enhanced by plasmons of Ag NP. As to our knowledge, optical and photoluminescent properties of Ag/Al₂O₃ nanocomposite films remain unstudied.

The nature of luminescence in Ag NP, clusters and composite nanostructures based on them is the matter of intensive discussions. A prevalent part of works is devoted to fluorescence of Ag nanoclusters, the minor one – to photoluminescence (PL) of Ag NP and nanostructures. In [4], the fluorescence spectrum of photoactivated AgO films contains five separate features (at 548, 594, 641, 673 and 725 nm) that are related with emission of Ag_n clusters (n = 2 – 8 atoms). In composite films Ag/TiO₂, emission with the wavelength close to 552 nm was explained by interband transitions in Ag₂O [2]. In alkaline glasses, containing Ag NP formed by thermal processing, present in PL spectra are both the band at 2.23 eV (ascribed to the interband transition in Ag₂O) and red bands with the energies lying below 2 eV and related with presence of small Ag NP [3]. But up to date, there is no information upon the luminescence relaxation times longer than several nanoseconds.

There exist wide opportunities to control photoluminescent and optical properties of silver NP as compared to those of gold, since their sizes, shape and surrounding can be controlled by formation of Ag_2O , AgO oxides with a set ratio between silver atoms and ions [2, 3, 6, 14]. The aim of this work is to prepare $\text{Ag}/\text{Al}_2\text{O}_3$ nanocomposite films by using the LPD method in vacuum, to study the influence of the silver concentration in target on extinction and time-resolved photoluminescence spectra as well as to ascertain interrelation between optical and photoluminescent properties of these films.

2. Experimental

Silver films and $\text{Ag}/\text{Al}_2\text{O}_3$ nanocomposite ones were prepared by the PLD method in vacuum chamber under the argon pressure 10–20 Pa. Deposition was carried out onto silicon and glass substrates. The silver films were prepared using forward and backward (high energy and low energy, respectively) particle flows from the erosion torch. $\text{Ag}/\text{Al}_2\text{O}_3$ nanocomposite films were deposited using the backward flow. The target consisted of small pieces of Al and Ag. The Ag concentration in the film was set by the ratio of areas of these pieces. The target was scanned by the $\text{YAG}:\text{Nd}^{3+}$ laser beam (wavelength 1.06 μm , pulse energy 0.2 J, pulse duration 10 ns, and repetition frequency 25 Hz). When depositing the films from the forward flow, the substrates were located normally to the torch axis at the distance 20–25 mm from the target. When using the backward flow, the substrates were located in the target plane. In the vicinity of the torch axis, the deposited nanoparticles were larger, far of the axis these were smaller. The thickness profile of the films was wedge-like within the range 500 down to 50 nm. The films prepared using the forward flow had no pores, rough, with grain dimensions up to hundreds nanometers, while those prepared using the backward flow were porous, smooth, with particle dimensions not exceeding tens nanometers.

Time-resolved PL spectra were measured within the energy range 1.4–3.2 eV with excitation by emission of a nitrogen laser (wavelength 337 nm, pulse duration 8 ns) and stroboscopic registration of signals in the photon-counting mode. The minimum strobe duration was 250 ns. Transmission spectra of the films were recorded using the spectrophotometer CФ-26 within the wavelength range 340–1000 nm.

3. Results and discussion

Shown in Fig. 1 are the transmission spectra of silver films (a) and those of $\text{Ag}/\text{Al}_2\text{O}_3$ nanocomposite films (b). It can be seen from Fig. 1a that all the silver films demonstrate clearly pronounced local surface plasmon absorption within the range 500–600 nm. At the same time, LSPR is extremely weak and practically is not observed in the nanocomposite films (Fig. 1b, curves 1–3) and can be seen only for the high (> 90 %) silver concentration in the target (Fig. 1b, curve 4).

Plasmon absorption in the nanocomposite films is slightly increased when exposing them to ambient air (compare curves 3 and 3' in Fig. 1b). The transmission minimum of the nanocomposite films is shifted to the blue range (415–430 nm) as compared to its position in the silver films. All the extinction spectra are broad, which is mainly related with dispersion of Ag NP sizes, shape and their surrounding.

Manifestation of LSPR in the silver films prepared using the forward particle flow from the erosion torch (Fig. 1a, curves 1 and 2) is caused by their rough surface. This fact was confirmed by an additional experiment checking the influence of the $\text{YAG}:\text{Nd}^{3+}$ laser beam ($\lambda = 1.06 \mu\text{m}$, free generation mode) on the target. Laser modification of its surface resulted in nanostructuring, which had an effect on the plasmon absorption spectrum (Fig. 1a, curves 1 and 2). In smooth films deposited from the backward flow, plasmon absorption is related with their porosity, with formation of a granulated structure (Fig. 1a, curves 3 and 4). In these films, with lowering the Ag NP sizes, in the film located at a great distance from the torch axis (Fig. 1a,

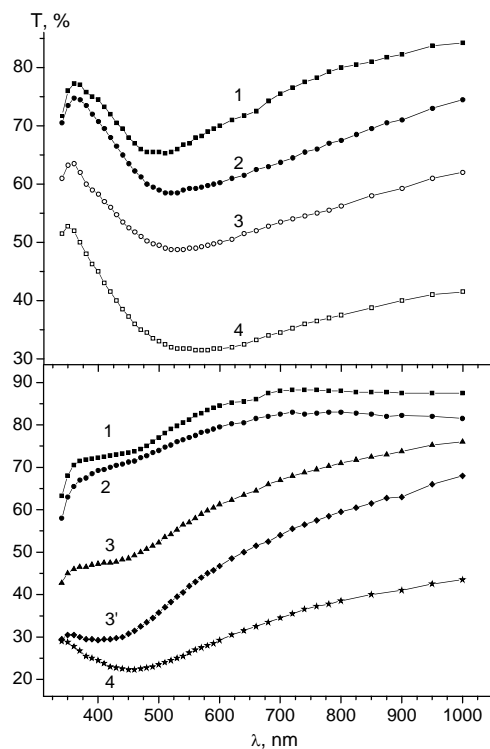


Fig. 1. Transmission spectra of the silver films (a) and $\text{Ag}/\text{Al}_2\text{O}_3$ nanocomposite films (b) prepared from forward (a, curves 1 and 2) and backward (a, curves 3, 4 and b) particle flows of the erosion torch under the following conditions of formation and measurements: - a, curve 2 – for the laser modified film (curve 1); - a, curves 3 and 4 – respectively for far and near points of the film from the torch axis; - b – for the films prepared with various silver concentrations in the target C_{Ag} , %: 1 – 20, 2 – 50, 3, 3' – 75, 4 – 90. The curve 3' – for the film (curve 3) after 3-day exposure to air.

curve 3) the transmission minimum is shifted to the short-wave side as compared with that in the film located near the torch (Fig. 1a, curve 4).

The observed optical properties of films, dependences of the intensity and energy positions for the plasmon resonance bands are inherent to NP of noble metals, since their extinction spectra depend on sizes, shape and surrounding of NP. The low LSPR efficiency is a distinctive feature of the optical properties of the films under investigation. We shall try to ascertain whether this fact is related with Landau decay, with losses of free electrons taking part in recombination processes.

Shown in Fig. 2 are time-resolved PL spectra of Ag/Al₂O₃ nanocomposite films that differ in their silver concentration C_{Ag} in the target during preparation. In the case of amorphous Al₂O₃ films ($C_{Ag} = 0$), we observed PL with a low intensity (I_{PL}) and relaxation times $\tau < 250$ ns (Fig. 2a, insert). Its spectra are broad, the band is located within the range 1.5 – 3.2 eV with the peak position close to 2.7 eV. Following the tradition, PL in Al₂O₃ films is related with emission of electron centers based on defect aggregates containing oxygen vacancies. PL is not observed in every silver film. It is explained by Coulomb electron-electron energy scattering, which is a faster process than radiative recombination.

On the contrary, all the nanocomposite films, even prepared with the lowest silver concentration in the target ($C_{Ag} = 1\%$) demonstrated PL (Fig. 2). As seen from this figure, photoluminescent properties of films strongly depend on preparation conditions. With increasing the C_{Ag} value, the PL spectrum is transformed, and the non-monotonic dependence of PL relaxation times is observed. Already at $C_{Ag} = 1\%$ the PL spectrum of films differs from that of Al₂O₃ films that do not contain Ag NP (Fig. 2a). There clearly pronounced are two peaks: narrower low-energy one at 1.6 eV and broader high-energy one within the range 2.2 – 3.0 eV. If the PL relaxation times in Al₂O₃ films were shorter than 250 ns, then in nanocomposite films with $C_{Ag} = 1\%$ they grow up to 500 ns.

With increasing the C_{Ag} value, the intensity of low-energy peak in PL spectra grows, and the shortwave shoulder of high-energy peak sharply constricts. When $C_{Ag} = 50\%$, the high-energy peak is approximately located at 2.2 eV (Fig. 2d, curve 1). When $C_{Ag} = 90\%$, the only shortwave shoulder remains (Fig. 2d, curve 2). The dependence of the relaxation time on C_{Ag} reaches its maximum at $C_{Ag} = 10\%$, and the relaxation time equals several microseconds (Fig. 2b). With further increase of C_{Ag} , the τ value is reduced: for $C_{Ag} = 20\%$ – $\tau = 500$ ns (Fig. 2c), and for $C_{Ag} > 50\%$ – $\tau < 250$ ns (Fig. 2d).

Our analysis of the PL kinetics for the film prepared with $C_{Ag} = 10\%$ shows that if within the time range $0 < \tau < 250$ ns one can observe a broad high-energy peak, then with increasing the relaxation time the latter sharply decreases, and for 750 ns $< \tau < 1$ μ s the only low-energy peak remains (Fig. 2b).

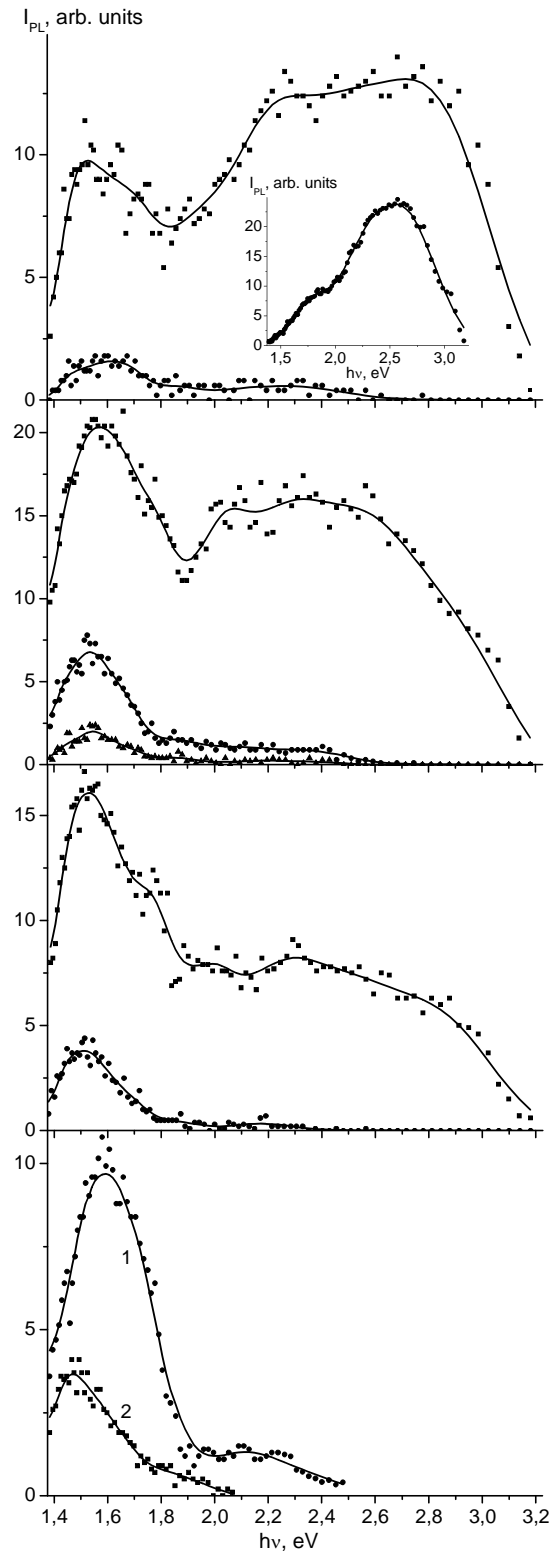


Fig. 2. Time-resolved photoluminescence spectra of Ag/Al₂O₃ nanocomposite films prepared with various Ag concentrations in the target C_{Ag} , %: a – 1, b – 10, c – 20; d, curve 1 – 50, d, curve 2 – 90. PL relaxation times for the top curves $\tau = 250$ ns, for the bottom ones: a, c – 250 ns $< \tau < 500$ ns, b – 750 ns $< \tau < 1000$ ns; d, curves 1, 2 – $\tau < 250$ ns. Insert in Fig. 2a – PL spectrum of the Al₂O₃ film, $\tau < 250$ ns.

We observed correlated changes in the PL intensity and relaxation time. The quantum efficiency of PL is lower than several percents. It is indicative of the fact that the PL efficiency is mainly determined by the degree of damping in the radiationless recombination channel. To ascertain the PL nature and recombination mechanisms needs further investigations. These can be related in the red range at short relaxation times with silver nanoclusters, the electron energy structure of which consists of discrete energy levels with respective interlevel transitions [3, 4]. PL in the spectral range close to 2.2 eV can be consistently explained by interband transitions in Ag₂O shell of Ag NP [2, 3]. Revealed for the first time in the prepared films the long PL relaxation times (up to several microseconds) cannot be explained by NP sizes within the simple free-electron model. Made in [10] are the attempts to relate them with the oxidized states of metal atoms, with interaction between metal ions and organic ligands, with complexes possessing hybridized states, with bands of charge transfer.

Juxtaposition of optical and photoluminescent properties of films is indicative of the fact that films possessing efficient PL do not display plasmon absorption. This confirms the assumption that damping the LSPR is related with leakage of free electrons from Ag NP that might display plasmon absorption. Instead, these electrons take part in recombination processes determining PL. Moreover, red PL does not excite plasmons in Ag NP, the absorption range of which lies in more shortwave range (< 600 nm).

4. Conclusion

The silver films and nanocomposite ones containing Ag NP in Al₂O₃ matrix were prepared using the method of pulsed laser deposition with forward and backward particle flows from the erosion torch. Local surface plasmon resonance was observed in the silver films and weakly pronounced in nanocomposite films prepared even at the high (close to 90 %) silver concentration in the target. Plasmon absorption in rough non-porous silver films is related with developed surface microrelief, while in the smooth porous ones – with the structure close to that in granulated films. PL is only inherent to nanocomposite films. PL spectra cover the broad spectral range 1.4 – 3.2 eV with the low-energy peak at approximately 1.6 eV and the high-energy one located within the range 2.2 – 2.7 eV. When the Ag concentration in the target grows, the intensity of the low-energy PL band grows, too. The measured relaxation times comprise the range 250 ns – 1 μs. In this work, we observed for the first time PL in the red spectral range with long relaxation times up to several microseconds. The dependence of the relaxation time on the Ag concentration in the target is non-monotonous and has its maximum at $C_{Ag} \sim 10\%$. The films that possess plasmon absorption do not display PL, and vice versa efficient PL is not inherent to the films where local surface plasmon resonance is clearly pronounced.

References

1. J.B. Pendry, L. Martin-Moreno, F.J. Garcia-Vidal, Mimicking surface plasmon with structured surface // *Science* **305**, p. 847-848 (2004)
2. H.M. Gong, S. Xiao, X.R. Su, J.B. Han, Q.Q. Wang, Photochromism and two-photon luminescence of Ag-TiO₂ granular composite films activated by near infrared ps/fs pulses // *Optics Express* **15**(21), p. 13924-13929 (2007).
3. P. Gangopadhyay, R. Kesavamoorthy, S. Bera, P. Magudapathy, K.G.M. Nair, B.K. Panigrahi, S.V. Narasimhan, Optical absorption and photoluminescence spectroscopy of the growth of silver nanoparticles // *Phys. Rev. Lett.* **94**, 047403(4) (2005).
4. L.A. Peyser, A.E. Vinson, A.P. Bartko, R.M. Dickson, Photoactivated fluorescence from individual silver nanoclusters // *Science* **291**, p. 103-106 (2001).
5. C.D. Geddes, A. Parfenov, I. Gryczynski, J.R. Lakowicz, Luminescent blinking from silver nanostructures // *J. Phys. Chem. B* **107**, p. 9989-19993 (2003).
6. T. Gleitsmann, B. Stegemann, T.M. Bernhardt, Femtosecond-laser-activated fluorescence from silver oxide nanoparticles // *Appl. Phys. Lett.* **84**, p. 4050-4052 (2004).
7. A.V. Aiboushev, A.A. Astafiev, Yu.E. Lozovik, S.P. Merkulova, V.A. Nadtochenko, O.M. Sarkisov, Enhanced luminescence of silver nanoclusters in mesoporous film // *Phys. Lett. A* **372**, p. 5193-5197 (2008).
8. A.A. Astafiev, Scanning near-field and two-photon microscopy of nano- and bioobjects // *Abstract of Cand. Thesis. Moscow* (2008) (in Russian).
9. H. Mertens, Controlling plasmon-enhanced luminescence // *Thesis of Ph.D FOM Institute for Atomic and Molecular Physics, Amsterdam, Netherlands* (2007).
10. J. Zheng, Fluorescent noble metal nanoclusters // *Thesis of Ph.D Georgia Institute of Technology, USA* (2005).
11. J.R. Lakowicz, K. Ray, M. Chowdhury, H. Szmajcinski, Yi Fu, J. Zhang, K. Nowaczyk, Plasmon-controlled fluorescence: a new paradigm in fluorescence spectroscopy // *Analyst* **133**, p. 1308-1346 (2008).
12. J.C.G. de Sande, R. Serna, J. Gonzalo, C.N. Afonso, D.E. Hole, A. Naudon, Refractive index of Ag nanocrystals composite films in the neighborhood of the surface plasmon resonance // *J. Appl. Phys.* **91**(3), p. 1536-1541 (2002).
13. K. Watonabe, K.H. Kim, D. Menzel, H.J. Freund, Hyperthermal chaotic photodesorption of xenon from alumina-supported silver nanoparticles: plasmonic coupling and plasmon-induced desorption // *Phys. Rev. Lett.* **99**, 225501(4) (2007).
14. G.I.N. Waterhouse, A. Graham, G.A. Bowmaker, J.B. Metson, The thermal decomposition of silver (I, III) oxide: a combined XRD, FT-IR and Raman spectroscopic study // *Phys. Chem. Chem. Phys.* **3**, p. 3838-3845 (2001).